Theory of interaction and bound states of spiral waves in oscillatory media

Igor S. Aranson
Racah Institute of Physics, The Hebrew University of Jerusalem, 91904 Jerusalem, Israel

Lorenz Kramer and Andreas Weber
Physikalisches Institut der Universität Bayreuth, Postfach 101251, 8580 Bayreuth, Germany
(Received 8 December 1992)

We present an alternative method for the calculation of the interaction between spirals in oscillatory media. This method is based on a rigorous evaluation of the perturbation of an isolated spiral resulting from neighboring spirals in a linear approximation. For the complex Ginzburg-Landau equation, the existence of bound states is identified with the parameter range where the perturbations behave in an oscillatory manner. The results for the equilibrium distance for two spirals in the bound state and also the dependence of the velocity of the spiral on the distance are in good agreement with numerical simulations. In the equally charged case, we find multiple bound states which may be interpreted as multiply armed spirals. Outside the oscillatory range, well-separated spirals appear to repel each other regardless of topological charge.

PACS number(s): 05.45.+b, 47.20.−k

I. INTRODUCTION

In spite of considerable effort, the problem of the interaction of defects in oscillatory media is not yet in a satisfactory state [1–3]. The simplest examples of such media are chemical oscillations such as the famous Belousov-Zhabotinskii reaction [4] or some cases of catalytic surface reactions [5]. The defects we are concerned with are the well-known spiral waves which are point defects in two dimensions (2D). More complicated examples of oscillatory media are systems sustaining (nonlinear) traveling waves as observed and/or predicted in thermal convection in binary fluids [6], homeotropically oriented nematic liquid crystals [7], and electroconvection in planarly aligned nematic liquid crystals [8]. The above defects correspond to dislocations in the roll pattern (for a general review see [9]). Transversely extended lasers are other systems where spiral-type defects occur [10].

The simplest description of such media is provided by the complex Ginzburg-Landau equation (CGLE)

$$\frac{\partial a}{\partial t} = a + (1 + ib)\Delta a - (1 + ic)|a|^2 a. \tag{1}$$

where the complex field a describes the amplitude and phase of the modulations of the pattern [11, 12]. This CGLE plays the role of a normal form in the vicinity of a supercritical transition to an oscillatory state in spatially extended systems and is thus very general. Many of the results obtained from the CGLE carry over qualitatively to situations where a more complicated description, e.g., by reaction-diffusion models, is more appropriate. This is true even for excitable media where, as in oscillatory systems, one has the existence of a continuous family of (phase) waves which does not, however, extend to zero wave number.

The simple zeros of a represent topologically stable point defects in 2D (and line defects in 3D). One has topological quantum numbers ± 1 related to the phase change of $\pm 2\pi$ when going around the defect. When $b - c \neq 0$ the defects are sources of spiral waves whose constant phase lines behave like an Archimedean spiral, except in the immediate neighborhood of the core. These spirals can give rise to very beautiful patterns [4] and seem to play an important role also in biological systems [13]. When $b - c$ tends to zero the emitted wave number goes to zero and the spirals go over into vortices which rotate if $b = c \neq 0$.

The asymptotic interaction is very different for the two cases: For $b - c = 0$ it is long-range decaying, essentially like r^{-1} with some corrections [14–17], whereas for $b - c \neq 0$ it is short-range decaying, essentially exponentially [1–3]. This latter behavior is easily understood: The waves emitted by the spiral screen the spiral core from perturbations arriving from outside. Interaction manifests itself in a motion of each spiral. The resulting velocity has a radial (along the line connecting the spiral cores) and a tangential component.

In Ref. [1] we presented detailed simulations of Eq. (1) for spiral pairs showing that a stable bound state exists at least for some values of the parameters with $|b-c|$ not too small. Up to now there exists no analytic understanding of the bound state and this problem will be addressed here.

The idea of the method used is actually quite straightforward: In full solutions for a spiral pair (or a more complicated aggregate of spirals) the spirals move with certain velocities and thus solutions exist only with the "correct" velocities. Such solutions may be constructed approximately by starting with isolated spirals, each one restricted to the region in space filled by its emitted waves and (small) velocities to be determined. For a spiral pair one simply has two half-spaces. The corrections are assumed to be determined to sufficient accuracy by the linearized problem with boundary conditions that take into

account the neighboring spiral. It is easily seen from the spectrum of the homogeneous part that bound states occur for $|b-c|$ above some threshold value ($c > c_{\rm cr} \approx 0.845$ for $b = 0$). The inhomogeneities involve the velocity linearly and as a consequence the solution for arbitrary (but not too small) distance can be expressed in terms of one inhomogeneous and one homogeneous solution. Once these are determined numerically and used to match the boundary conditions, the velocity versus distance relation comes out.

This program is carried through in Secs. II–IV for oppositely (or "unlike-") charged spirals and $b = 0$ (for simplicity) and $c > c_{\rm cr}$, where one has a sequence of bound states, i.e., states with zero radial velocity. There remains a tangential velocity leading to a drift of the pair. In Sec. V we consider the case $c < c_{\rm cr}$ (no bound states), discuss the generalization to $b \neq 0$, connect with the results for $b-c = 0$, and finally generalize to like- (or equally) charged spirals. We argue that for sufficiently large separation, the velocity versus distance relations are similar to the previous case except that the tangential velocities of the two spirals are now opposite each other. Then bound spirals rotate around each other and can be interpreted as a doubly charged spiral. We also present numerical simulations with more than two charges.

II. THE PROBLEM OF INTERACTION

The (one-armed or singly charged) isolated spiral solution of Eq. (1) is of the form

$$\tilde{a}(r,\theta) = F(r)\exp\{i[\omega t \pm \theta + \psi(r)]\} \tag{2}$$

and satisfies the following equations for the functions $F(r)$ and $\psi(r)$:

$$\begin{aligned} &\Delta_r F - \frac{1}{r^2}F - (\psi')^2 F \\ &\qquad -b[(\Delta_r\psi)F + 2\psi' F'] + F - F^3 = 0, \\ &b\left(\Delta_r F - \frac{1}{r^2}F - (\psi')^2 F\right) \\ &\qquad +(\Delta_r\psi)F + 2\psi' F' - \omega F - cF^3 = 0, \end{aligned} \tag{3}$$

where (r,θ) are polar coordinates, $\Delta_r = \partial_r^2 + \frac{1}{r}\partial_r$, and primes denote derivatives with respect to r. The functions F and ψ have the following asymptotic behavior:

$$\begin{aligned} &F(r) \to \sqrt{1-k^2}, \quad \psi'(r) \to k, \quad r \to \infty \\ &F(r) \sim r, \quad \psi'(r) \sim r, \quad r \to 0 \end{aligned} \tag{4}$$

and $\omega = -bk^2 - c(1-k^2)$. The constant k is the asymptotic wave number of the waves emitted by the spiral, which is determined uniquely for given b, c. In general k has to be determined numerically (see, e.g., [18, 16]).

Due to the interaction with other spirals or with a boundary, the spiral core moves with some velocity $\mathbf{v}$, which is to be calculated. We associate with each spiral a region determined by the wave emitted by the spiral. Thus, in an infinite system the boundaries are given by the shocks that build up where the waves of neighboring spirals collide. Inside each region the perturbed spiral solution is written in the form

$$a(r,\theta) = [F(r) + W(r,\theta,t)]\exp\{i[\omega t + \theta + \psi(r)]\}, \tag{5}$$

where W is the correction to the unperturbed spiral solution and r, θ are now the coordinates comoving with the velocity v. For definiteness of the analysis we have chosen the + sign in Eq. (2). If the spirals are well separated one can expect the correction function W to be small, except maybe in the region of the shock between spirals. Our results demonstrate that the corrections are indeed rather small. Hence the correction can be determined in principle from the linear approximation. (The linearization can in principle be avoided, but the problem becomes more complicated.)

The function W obeys the system of equations (we focus again on one spiral; the domain is now the half-plane)

$$\begin{aligned} &-\mathbf{v}\nabla W - W_t - i\{\mathbf{v}\nabla[\theta + \psi(r)]\}W + (1+ib)\left[\Delta W - \frac{1}{r^2}W - (\psi')^2 W + i\Delta_r\psi W + 2i\left(\psi' W' + \frac{1}{r^2}\partial_\theta W\right)\right] \\ &\qquad +(1-i\omega)W - (1+ic)F^2(2W + W^*) = v\left[\left(F'\sin(\theta+\eta) + i\psi' F\sin(\theta+\eta) + i\frac{F}{r}\cos(\theta+\eta)\right)\right], \end{aligned} \tag{6}$$

where $\mathbf{v} = (v_x, v_y)$ is the velocity and $\eta = \arctan(v_x/v_y)$. The exact Eq. (6) also contains, on the left-hand side, the terms $-(1+ic)[F(W^2 + 2|W|^2) + |W|^2 W]$, which we neglect in linear approximation. We have used

$$\begin{aligned} \frac{\partial\tilde{a}}{\partial t} = v_y\partial_y\tilde{a} + v_x\partial_x\tilde{a} + i\omega\tilde{a} = \Big(&F'(v_y\sin\theta + v_x\cos\theta) + i\psi' F(v_y\sin\theta \\ &+v_x\cos\theta) + i\frac{F}{r}(v_y\cos\theta - v_x\sin\theta) + i\omega F\Big)\exp\{i[\omega t + \theta + \psi(r)]\}. \end{aligned} \tag{7}$$

For simplicity we now consider two spirals located on the x axis at $\pm X$. The problem of the interaction of two oppositely charged or like-charged spirals is equivalent to the problem of the interaction of one spiral with a plane boundary with different boundary conditions. In the case of oppositely charged spirals the symmetry of a problem is $a(x,y) = a(-x,y)$. Numerically obtained bound states of oppositely charged spirals indeed possess such a symmetry (see Fig. 1). Here the term "bound state" means that the distance between the spiral cores is in stable equilibrium, but there is drift in the y direction.

For this case, therefore, the boundary conditions at $x = 0$ are

$$\frac{\partial a}{\partial x} = 0. \tag{8}$$

Then the velocities of the spirals obey the relation $v_{1x} = -v_{2x}$ and $v_{1y} = v_{2y}$. Presumably, in this case there is no additional time dependence in the correction function W. The case of like-charged spirals is more complicated because the symmetry of the problem is $a(x,y) = a(-x,-y)$ and the velocities obey $v_{1x} = -v_{2x}, v_{1y} = -v_{2y}$. However, in Sec. V we show that this case is in some approximation also similar to the oppositely charged spirals. A snapshot of a bound state of two like-charged spirals is shown in Fig. 2; there spirals rotate around each other.

We suppose that the velocity of the spiral drift v is small, which is the case when the distance $2X$ between the spirals is large. The condition $vX \ll 1$ will also be

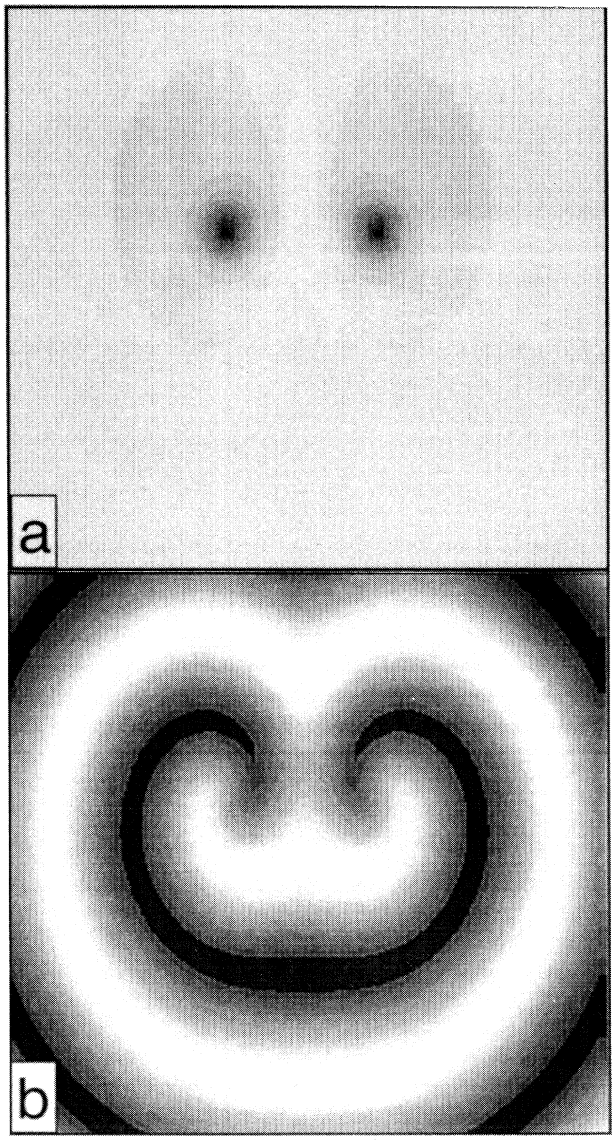

FIG. 1. The bound state of oppositely charged spirals for $b = 0, c = 1.5$ in a 100×100 domain. Represented: (a) $|a(x,y)|$; (b) real part $\mathrm{Re}a(x,y)$. Snapshot is coded in the grey scale, maximum of the field corresponds to black, minimum to white.

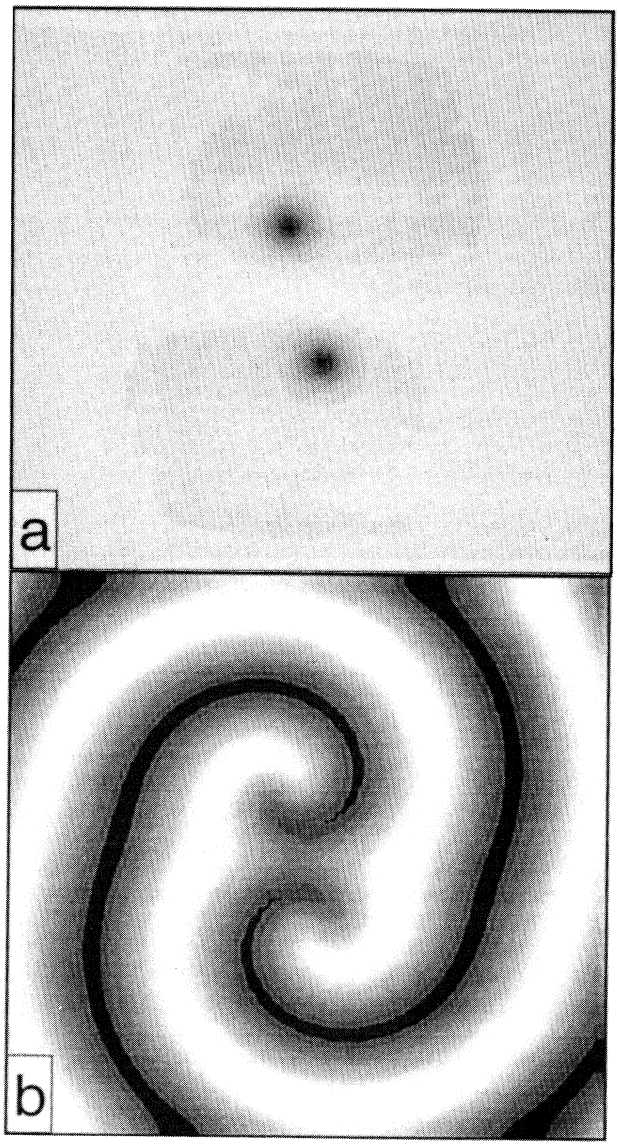

FIG. 2. The bound state of two like-charged spirals for $b = 0, c = 1.5$ in a 50×50 domain. Represented: (a)$|a(x,y)|$; (b) $\mathrm{Re}a(x,y)$.

needed and it turns out to be satisfied for well-separated spirals. The terms $\sim vW$ in Eq. (6) can be omitted in the general case $b \neq c$ because it involves two small quantities, but they become important for $b = c$ (see Sec. V). Also, the solution presented below has no explicit time dependence, so W_t will be dropped.

Equation (6) can be simplified by using Eqs. (3). This gives

$$(1+ib)\left\{\Delta W - \frac{\Delta_r F}{F}W + 2i\left[\psi' F\frac{\partial}{\partial r}\left(\frac{W}{F}\right) + \frac{1}{r^2}\partial_\theta W\right]\right\} - (1+ic)F^2(W+W^*)$$

$$= v\left(F'\sin(\theta+\eta) + i\psi' F\sin(\theta+\eta) + i\frac{F}{r}\cos(\theta+\eta)\right). \quad (9)$$

From now on we restrict ourselves to the case $b = 0$ to avoid lengthy expressions. The generalization to the case of arbitrary b is discussed in Sec. V. Now, separating the real and the imaginary parts of $W = A + iB$ gives the pair of equations

$$\Delta A - 2F^2 A - \frac{\Delta_r F}{F}A - 2\left[\psi' F\frac{\partial}{\partial r}\left(\frac{B}{F}\right) + \frac{1}{r^2}\partial_\theta B\right] = vF'\sin(\theta+\eta),$$

$$\Delta B - 2cF^2 A - \frac{\Delta_r F}{F}B + 2\left[\psi' F\frac{\partial}{\partial r}\left(\frac{A}{F}\right) + \frac{1}{r^2}\partial_\theta A\right] = v\left(\psi' F\sin(\theta+\eta) + \frac{F}{r}\cos(\theta+\eta)\right). \quad (10)$$

The solution of Eqs. (10) can be represented in the form of a Fourier series

$$\begin{pmatrix} A \\ B \end{pmatrix} = \sum_{n=-\infty}^{\infty}\begin{pmatrix} A_n(r) \\ B_n(r) \end{pmatrix}\exp(in\theta) \quad (11)$$

together with the condition

$$A_n = A^*_{-n}, \quad B_n = B^*_{-n}. \quad (12)$$

Equations (10) then become

$$\Delta_r A_n - \frac{n^2}{r^2}A_n - 2F^2 A_n - \frac{\Delta_r F}{F}A_n$$

$$-2\left[\psi' F\frac{\partial}{\partial r}\left(\frac{B_n}{F}\right) + \frac{in}{r^2}B_n\right]$$

$$= \frac{vn}{2i}F'\delta_{\pm 1,n}\exp(in\eta), \quad (13)$$

$$\Delta_r B_n - \frac{n^2}{r^2}B_n - 2cF^2 A_n - \frac{\Delta_r F}{F}B_n$$

$$+2\left[\psi' F\frac{\partial}{\partial r}\left(\frac{A_n}{F}\right) + \frac{in}{r^2}A_n\right]$$

$$= \frac{v}{2}\left(-in\psi' F + \frac{F}{r}\right)\delta_{\pm 1,n}\exp(in\eta).$$

The dominant contributions come from the terms with $|n| \leq n_c$, where the constant $n_c \sim \sqrt{X}$ (see below). The velocity enters only into the equations for $n = \pm 1$. We consider separately the behavior of the solutions of Eq. (13) for $r \to 0$ and for $r \to \infty$. Equation (10) [or equivalently Eqs. (13)] together with appropriate boundary conditions is solvable only for a distinct velocity depending on the spiral separation.

III. ASYMPTOTIC BEHAVIORS

A. $r \gg 1$

Consider the behavior of the homogeneous solutions ($v = 0$) of Eqs. (13) for $r \to \infty$ (the results will be applicable also for $v \neq 0$ because the relevant homogeneous solutions diverge and always dominate asymptotically). Then we can neglect the terms $\sim \Delta_r F$, $1/r$, and $1/r^2$. Also we can replace ψ' by k and F by $\sqrt{1-k^2}$. Then one has the simplified system for arbitrary n

$$A_n'' - 2(1-k^2)A_n - 2k\partial_r B_n = 0,$$

$$B_n'' - 2c(1-k^2)A_n + 2k\partial_r A_n = 0, \quad (14)$$

describing perturbations of the asymptotic plane waves emitted by the spiral. Substituting the solution in the form $A_n, B_n \sim \exp(pr)$, we have the following characteristic equation:

$$p\{p^3 + p[4k^2 - 2(1-k^2)] - 4ck(1-k^2)\} = 0. \quad (15)$$

The root $p_0 = 0$ corresponds to the translation mode. Using the numerically defined asymptotic spiral wave number k it turns out that for $c > c_{cr} \approx 0.845$ the equation possesses one real negative root $p_3 < 0$ and a pair of complex-conjugate roots $p_{1,2} = \alpha \pm i\beta$ with $\alpha > 0$. In contrast, for $c < c_{cr}$ all the roots are real. It will be shown later that the value $1/\beta$ defines the distance between the spirals in the bound state. For $c < c_{cr}$ there is no bound state.

A more detailed analysis including $O(r^{-1})$ corrections

to Eq. (13) shows that the asymptotic solutions are given by

$$\begin{pmatrix} A_n \\ B_n \end{pmatrix} = r^{\mu} \begin{pmatrix} 1 \\ \gamma \end{pmatrix} \exp(pr) \tag{16}$$

with

$$\gamma = \frac{p^2 - 2(1-k^2)}{2pk}, \qquad \mu = \frac{4k^2 - 2p^2 + 6kp/c}{3p^2 + 6k^2 - 2}. \tag{17}$$

Obviously, the factor $\sim r^{\mu}$ is slowly varying in comparison with the exponent for $r \gg 1$, but it turns out to be important to get good quantitative results. Thus, for $c > c_{\rm cr}$ (we consider first this case) the outer solution of Eqs. (10) is of the form

$$\begin{pmatrix} A \\ B \end{pmatrix} = \sum_{n=-\infty}^{\infty} \left[\begin{pmatrix} 1 \\ \gamma \end{pmatrix} C_{1n} r^{\mu} \exp(pr) + \begin{pmatrix} 1 \\ \gamma^* \end{pmatrix} C_{2n} (r^{\mu})^* \exp(p^* r) \right] \exp(in\theta) \tag{18}$$

with $C_{1n} = C^*_{2,-n}$ and $p = p_1$.

The coefficients C_{1n}, C_{2n} are to be determined from the boundary conditions for $x = 0$. From Eq. (8) (oppositely charged spirals) we have

$$\frac{\partial a(r,\theta)}{\partial x} = [F_x + W_x + i(F+W)(\psi_x + \theta_x)] \times \exp[i(\theta + \psi + \omega t)] = 0. \tag{19}$$

For $r \gg 1$ one can neglect F_x, θ_x and then the equation simplifies considerably

$$W_x + i\psi_x W = -i\psi_x F. \tag{20}$$

Also, for $r \gg 1$ one can use $\psi_x \approx k\cos\theta, W_x \approx W' \cos\theta$, and $F \approx \sqrt{1-k^2}$. Then we obtain

$$W' + ikW = -ik\sqrt{1-k^2}. \tag{21}$$

Separating Eq. (21) into real and imaginary part one arrives at

$$A' - kB = 0\ , \quad B' + kA = -k\sqrt{1-k^2}. \tag{22}$$

Now, substituting (18) into (22) leads to the following equations for the coefficients:

$$\sum_{n=-\infty}^{\infty} \left[\begin{pmatrix} p - k\gamma \\ p\gamma + k \end{pmatrix} C_{1n} r^{\mu} \exp(pr) + \begin{pmatrix} p^* - k\gamma^* \\ p^*\gamma^* + k \end{pmatrix} C_{2n} (r^{\mu})^* \exp(p^* r) \right] \exp(in\theta) = \begin{pmatrix} 0 \\ -k\sqrt{1-k^2} \end{pmatrix}. \tag{23}$$

On the boundary the radius r depends on the angle θ as

$$r(\theta) = \begin{cases} \frac{X}{\cos\theta}, & -\frac{\pi}{2} < \theta < \frac{\pi}{2} \\ \infty, & |\theta| > \frac{\pi}{2}. \end{cases} \tag{24}$$

The C_{2n} can be eliminated from Eq. (23) leading to

$$\sum_{n=-\infty}^{\infty} C_{1n} \exp(in\theta) = -k\frac{\sqrt{1-k^2}}{\delta} \exp(-pr) r^{-\mu}, \tag{25}$$

where the constant δ is

$$\delta = p\gamma + k - (p^*\gamma^* + k)\frac{p - k\gamma}{p^* - k\gamma^*}\ . \tag{26}$$

For $x = 0$ we can expand $\exp(-pr)r^{-\mu}$ in the series

$$\exp[-pr(\theta)] r(\theta)^{-\mu} = \sum_{n=0}^{\infty} Z_n \cos(n\theta), \tag{27}$$

where

$$Z_n = 2\frac{1}{\pi} \int_{-\pi}^{\pi} \exp\left(-p\frac{X}{\cos(\theta)}\right) \cos(n\theta) \left(\frac{X}{\cos\theta}\right)^{-\mu} d\theta. \tag{28}$$

From Eqs. (25) and (27) one has $C_{1,-n} = C_{1,n}$ from which it follows that $C_{1,n} = C^*_{2,n}$. For $X \gg 1$ the coefficients Z_n can be estimated easily because the main contribution to the integrals comes from the region of small θ. For $\theta \ll 1$ we can replace in the exponent $X/\cos(\theta) \approx X(1 + \theta^2/2)$. After simple algebra we have

$$Z_n = \frac{\exp(-pX)}{\sqrt{\pi pX/2}} X^{-\mu} \exp(-n^2/2pX). \tag{29}$$

Equations (25), (27), and (29) now give ($n \neq 0$)

$$C_{1n} = C^*_{2n} = -\frac{k\sqrt{1-k^2}\exp(-pX)}{\delta\sqrt{2\pi pX}} X^{-\mu} \exp(-n^2/2pX). \tag{30}$$

Clearly for $n^2 < 2|p|X$ the last exponent can be omitted. Actually, to obtain the results shown futher on the integrals (28) were used directly instead of the approximations (29). The differences turned out to be small.

B. $r \to 0$

From now on we only need to consider the contributions from $n = 1$ so we omit the subscript n. Consider the solutions of Eqs. (13) for $r \to 0$ and $n = 1$. We shall analyze the homogeneous solutions ($v = 0$), but again the results are applicable to the case $v \neq 0$. Because $F \sim r$, $\psi \sim r$, and $\Delta F/F \to 1/r^2$ for $r \to 0$, Eqs. (13) reduce as follows:

$$A'' + \frac{1}{r}A' - \frac{2}{r^2}A - \frac{2i}{r^2}B = 0, \qquad B'' + \frac{1}{r}B' - \frac{2}{r^2}B + \frac{2i}{r^2}A = 0. \tag{31}$$

We can look for the solution of (31) in the form

$$\begin{pmatrix} A \\ B \end{pmatrix} \sim \begin{pmatrix} a_m \\ b_m \end{pmatrix} r^m, \tag{32}$$

and this leads to $m = \pm 2$ or $m = 0$. In the case $m = 0$ the behavior $\sim \ln r$ is also admitted. The homogeneous solution of Eqs. (13) corresponding to the translation mode for the spiral is given by

$$\begin{pmatrix} A_t \\ B_t \end{pmatrix} = \begin{pmatrix} F' \\ iF/r + \psi' F \end{pmatrix}. \tag{33}$$

For $r \to 0$ it reduces to the solution (32) with $m = 0$ and no logarithmic term. For $r \to \infty$ it is bounded and therefore not essential for our analysis. The solutions of Eqs. (13) with the other allowed behavior for $r \to 0$ are expected to behave for $r \to \infty$ according to Eq. (18).

IV. DETERMINATION OF THE VELOCITIES

A. General procedure

If the velocity $\mathbf{v}$ is chosen zero, then it is impossible to satisfy the boundary conditions (30) for $r \to \infty$ and regularity for $r \to 0$ simultaneously. Only the proper choice of the velocity $\mathbf{v}$ allows to satisfy both conditions.

The following procedure can be employed. One determines (numerically) a particular inhomogeneous solution of Eqs. (13) for $n = 1$ with zero initial conditions for $r = 0$

$$A(0) = B(0) = A'(0) = B'(0) = 0, \tag{34}$$

leading to a solution which is regular at $r = 0$. Actually, a more general case of the initial conditions could be $A(0) = iB(0)$=const, $A'(0) = B'(0) = 0$, but from our point of view this solution is equivalent to the solution (34) because it differs only by the trivial bounded solution (33). From the linearity of Eqs. (13) in $\mathbf{v}$ one sees that a solution for arbitrary value of $\mathbf{v}$ can be obtained by superposition of solutions with $v_x = 1, v_y = 0$ and $v_x = 0, v_y = 1$, which is equivalent to $v = 1$ with $\eta = 0$ and $\eta = \pi/2$, respectively. For $r \to \infty$ the solutions behave according to Eq. (18) and we obtain the constants C_{1x}, C_{2x} (for $v_x = 1, v_y = 0$) and C_{1y}, C_{2y} (for $v_x = 0, v_y = 1$). Actually, one needs to compute only one case because from Eqs. (13) one has the relation $C_{1x} = iC_{1y}, C_{2x} = iC_{2y}$. In general the relations $C_{1x} = C^*_{2x}$ and $C_{1y} = C^*_{2y}$ are not satisfied [first boundary condition (30)]. To correct this it is useful to determine (numerically) a homogeneous solution of Eqs. (13) that behaves as (32) with $m = 2$ for $r \to 0$ and compute the asymptotic constants C_1, C_2. Then the superposition satisfying the first boundary condition (30) are determined (mixing factors ξ_x, ξ_y) leading to

$$\begin{aligned} C_x &= C_{1x} + \xi_x C_1 = C^*_{2x} + \xi^*_x C^*_2, \\ C_y &= C_{1y} + \xi_y C_1 = C^*_{2y} + \xi^*_y C^*_2. \end{aligned} \tag{35}$$

Thus for each value of the parameter c the constants C_x, C_y are uniquely determined. Then v_x and v_y may be calculated as a function of distance X by satisfying the second condition (30),

$$C_{11}(\mathbf{v}) = v_x C_x + v_y C_y = -\frac{k\sqrt{1-k^2}\exp(-pX)}{\delta\sqrt{2\pi pX}} X^{-\mu}. \tag{36}$$

One easily sees from (36)

$$v_x = \mathrm{Im}\left(\frac{-k\sqrt{1-k^2}\exp(-pX)}{\delta C_y\sqrt{2\pi pX}} X^{-\mu}\right) \Big/ \mathrm{Im}(C_x/C_y), \tag{37}$$

$$v_y = \mathrm{Re}\left(\frac{-k\sqrt{1-k^2}\exp(-pX)}{\delta C_y\sqrt{2\pi pX}} X^{-\mu}\right) - v_x \mathrm{Re}(C_x/C_y).$$

The bound states of the CGLE correspond to the case of $v_x = 0$. Therefore the equilibrium distance $2X_e$ can be founded from the equation

$$\mathrm{Im}\left(\frac{-k\sqrt{1-k^2}\exp(-pX_e)}{\delta C_y\sqrt{2\pi pX_e}} X_e^{-\mu}\right) = 0. \tag{38}$$

From (38) we have the expression

$$\mathrm{Im}[pX_e + \mu \ln X_e] = -\phi + \pi l, \tag{39}$$

where $l = 1, 2, 3, \ldots$ and $\phi = -\arg[1/(\delta C_y p^{1/2})]$. One thus needs only one solution of Eqs. (13) in order to determine the velocities for all distances.

B. Numerical methods

For the solution of the linearized problem Eqs. (13) for $n = 1$ we used the following method. First for each fixed value of c we obtained the unperturbed spiral solution from Eqs. (3). We used here a very fine discretization ($\Delta r = 0.01$) to reproduce the characteristics of the spiral with high accuracy. Then we solved Eqs. (13) using these solutions. The main difficulty here is the divergence of the coefficients in Eqs. (13) for $r \to 0$. To control this singularity we developed a special numerical method based on the use of the exact Green's functions of the problem for $r \to 0$. The idea of the method is the following. For $m = 0$ [compare Eq. (32)] Eqs. (13) can be represented in the form

$$A'' + \frac{1}{r}A' = f_1\ , \quad B'' + \frac{1}{r}B' = f_2, \tag{40}$$

where the functions $f_{1,2}$ are regular for the solutions with $m = 0$. The solutions of (40) [and therefore (13)] are of the form

$$\begin{aligned} A(r) &= D_1 + D_2 \ln r + \int_0^r \frac{dr_1}{r_1} \int_0^{r_1} r_2 f_1 dr_2, \\ B(r) &= G_1 + G_2 \ln r + \int_0^r \frac{dr_1}{r_1} \int_0^{r_1} r_2 f_2 dr_2. \end{aligned} \tag{41}$$

As initial conditions we have chosen $D_{1,2} = G_{1,2} = 0$, and evaluated the integrals on the right-hand side of (41) between grid points by the trapezium method. Similarly, for $m = 2$ we have the system

$$A'' + \frac{1}{r}A' - \frac{4}{r^2}A = f_3,$$
$$B'' + \frac{1}{r}B' - \frac{4}{r^2}B = f_4, \tag{42}$$

and the corresponding solution in the form

$$A(r) = D_1 r^2 + D_2 r^{-2} + \int_0^r \frac{dr_1}{4r_1} r^2 [1 - (r_1/r)^4] f_3,$$
$$B(r) = G_1 r^2 + G_2 r^{-2} + \int_0^r \frac{dr_1}{4r_1} r^2 [1 - (r_1/r)^4] f_4. \tag{43}$$

As initial conditions one may choose $D_2 = G_2 = 0$ and $D_1 = -iG_1 = 1$. To extract from the solution of Eqs. (40) and (42) the coefficients $C_{1,2}$ we just use the expressions (18).

C. Comparison with results of numerical simulations

The full simulations of Eq. (1) were carried out on a CRAY YMP Supercomputer. We used a second-order quasispectral method based on a fast Fourier transform (FFT). The typical values of the parameters of the code were as follows: the number of harmonics in each direction was 256, the system size was 100×200 dimensionless units, and the time step $\Delta\tau \sim 0.1$. The results were checked with better space discretization and smaller time steps. The simulations were carried out under periodic boundary conditions (because of the use of FFT) with total topological charge in the elementary cell equal to zero. To reproduce nonflux boundary conditions (zero normal derivative on the boundary) relevant for oppositely charged spirals, the elementary cell was divided into four equal quadrants. Computations were performed only in one quadrant and extended by symmetric reflection at the boundary lines. Initializing one spiral then means that in fact there are four spirals in the elementary cell with alternating topological charge as one goes around the quadrants. If the domain is large enough, and the spiral is placed near one of the boundaries, it experiences effectively only one image spiral because the distance to the rest is much larger. For like-charged spirals we extended the field by reflection at the middle point of the boundary line so that one here has a like-charged pair. Extension to the other half of the elementary cell was again by (symmetric) reflection at the remaining boundaries so that one has there another like-charged pair with charges opposite the first pair. Such symmetrization of the field was performed on each time step to avoid the accumulation of numerical errors (although in principle it is enough to set the symmetry once in the initial conditions).

In Fig. 3 the dependence of the velocities on the spiral separation X is plotted for $b = 0, c = 1$ and compared with results from full numerical simulations. There is reasonable agreement, particularly for the radial velocity V_x. The first zero of v_x at $2X_e \approx 11.5$ corresponds to $l = 1$ in Eq. (39). The next zero at $2X_e \approx 22.8$ corresponds to a stable bound state. Here the velocities are already extremely small. From the simulations no other bound state could be resolved.

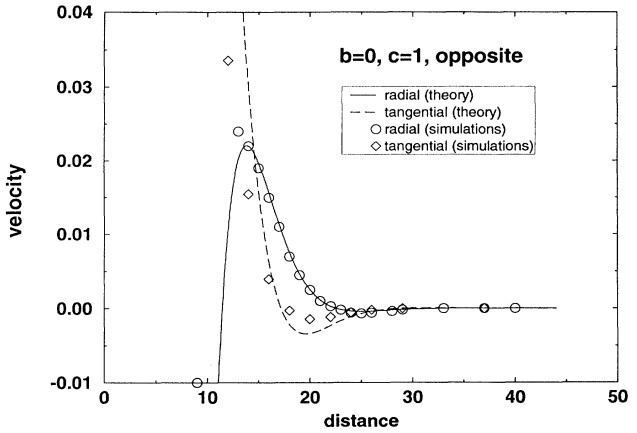

FIG. 3. The dependence of radial (v_x) and tangential (v_y) velocities on the spiral separation $2X$ for $b = 0, c = 1$.

The equilibrium distance obtained from the theory [$l = 2$ in Eq. (39)] is in very good agreement with the results of the simulations of the full CGLE [see Fig. 4(a)].

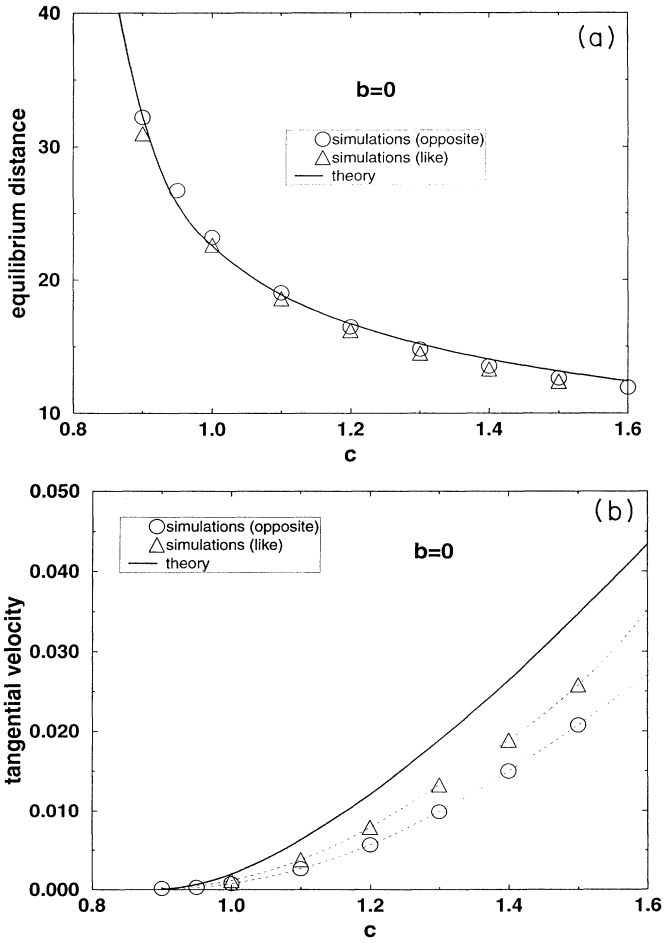

FIG. 4. The comparison of the parameters of bound state with the results of simulations of Eq. (1). (a) Equilibrium distance $2X_e$ given by Eq. (39) as function of c for $b = 0$; (b) tangential velocity v_y at the equilibrium distance for $b = 0$.

Nevertheless, there is some disagreement between the values of tangential velocity v_y by a factor of about 1.5 [see Fig. 4(b)], although the dependence on c is very similar. We can offer the following explanation.

The first reason is basically technical. Actually, the small absolute errors in the determination of the equilibrium distance lead to large relative errors in tangential velocity because of the exponential dependence on X. In our theoretical results the equilibrium distance is in most cases slightly smaller than in the simulations. Increase of the distance changes the velocity in the right direction.

The second reason could be the contribution from nonlinear terms which we dropped in Eq. (6). Formally speaking, for $c \sim 1$ they are not too small. Possibly these terms change slightly the value of the equilibrium distance, which leads to an increase of the velocity. Also $1/X$ corrections to the boundary condition (20) could improve the results.

V. GENERALIZATIONS

A. $c \leq c_{cr}$

In the case $0 < c < c_{cr}$ we have two real positive roots of Eq. (15), for definiteness $0 < p_1 < p_2$. Therefore the outer solution is now of the form

$$\begin{pmatrix} A \\ B \end{pmatrix} = \sum_{n=-\infty}^{\infty} \left[\begin{pmatrix} 1 \\ \gamma_1 \end{pmatrix} C_{1n} r^{\mu_1} \exp(p_1 r) + \begin{pmatrix} 1 \\ \gamma_2 \end{pmatrix} C_{2n} r^{\mu_2} \exp(p_2 r) \right] \exp(in\theta), \tag{44}$$

where $\gamma_{1,2}$ and $\mu_{1,2}$ are given by expressions analogous to Eqs. (17). In the same way as before one arrives at expressions analogous to Eq. (30). Applying the analysis as in the preceding sections, we can derive from the boundary conditions the expressions for the coefficients C_{in}. They are of the form

$$C_{in} = -\frac{k\sqrt{1-k^2}\exp(-p_1 X)}{\delta_i \sqrt{2\pi p_1 X}} X^{-\mu_i} \exp(-n^2/2p_i X). \tag{45}$$

The constants $\delta_{1,2}$ are defined in analogy to (26). Using the analogous numerical procedure one can also determine the constants $C_{x,y}$, but for small c it is technically very difficult in this form [for $r \to \infty$ the dominant contribution in (44) is caused by the term with the leading exponent p_2]. In the general case $0 < c < c_{cr}$ the velocities $v_{x,y}$ depend on both exponents $\exp(-p_1 X), \exp(-p_2 X)$.

The results can be simplified considerably for the case $c \to 0$ and $|ck|X \gg 1$. Then one can neglect the coefficients C_{2n} because for $c \to 0$ one has $0 < p_1 \approx -2ck \ll 1$, $p_2 \approx \sqrt{2}$, $\mu_1 \to 0$, and $\delta_1 \to -1/(2k)$. Therefore we have from the boundary conditions

$$C_{1n} = \frac{k^2 \exp(-|2ck|X)}{\sqrt{\pi |ck| X}}, \quad C_{2n} = 0. \tag{46}$$

After the matching with the solution for $r \to 0$ we will obtain the result $v_{x,y} \approx C_{x,y}^{-1} \exp(-2|ck|X)/\sqrt{X}$. This coincides with an earlier analysis using a phase diffusion equation [1–3]. From the numerical simulations for $b = 0$ and $c = 0.5$, shown in Fig. 5, one finds $C_x > 0$ leading to asymptotic repulsion. This can be inferred already from the work of Biktashev [3], who used a phase-diffusion equation and asymptotic matching to treat the interaction of spirals with a boundary. Figure 5 also shows that the interaction becomes attractive at smaller distance leading to final annihilation of the spiral pair. Our results appear to be in contradiction with the work [2], where in the limit $c \to 0$ matching with the internal solution was done analytically. In this situation simulations with smaller values of c would seem useful, but they are too time consuming. Note that for $b = 0, c = 0.5$ one has already a rather small $|k|$ (≈ 0.08). The repulsive range is expected to move to larger X roughly as $|ck|^{-1}$ for smaller c.

B. The case of $b \neq 0$

It is well known that the homogeneous equation (9) admits a similarity transformation from the case $b \neq 0$ to the case $b = 0$ [18, 16]. Indeed, dividing the equation by $(1 + ib)$ and performing the following transformations of the variables:

$$\begin{aligned} \tilde{c} &= \frac{c-b}{1+bc}, \\ \tilde{k} &= \frac{k}{\sqrt{(1-\omega b)/(1+b^2)}}, \\ \tilde{r} &= r\sqrt{(1-\omega b)/(1+b^2)}, \\ \tilde{\omega} &= \frac{\omega + b}{1-\omega b}, \\ \tilde{F} &= F\sqrt{\frac{1+bc}{1-\omega b}} \end{aligned} \tag{47}$$

leads to the case $b = 0$, but with a new value of c. There-

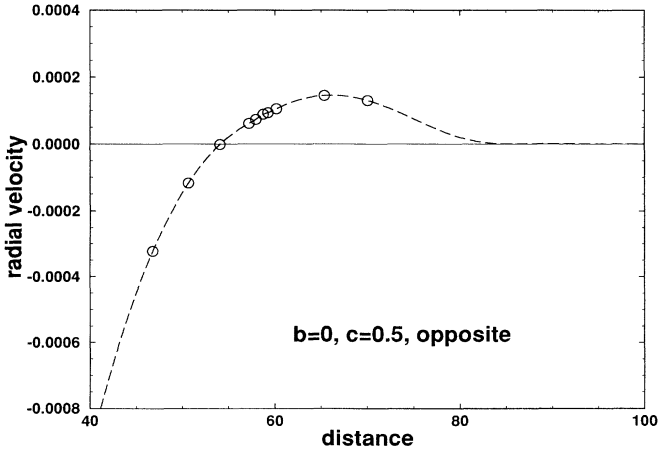

FIG. 5. The dependence of the velocity v_x on the spiral separation $2X$ for $b = 0, c = 0.5$ [results of simulations of Eq. (1)]. The relative errors are about 15% in the repulsive range.

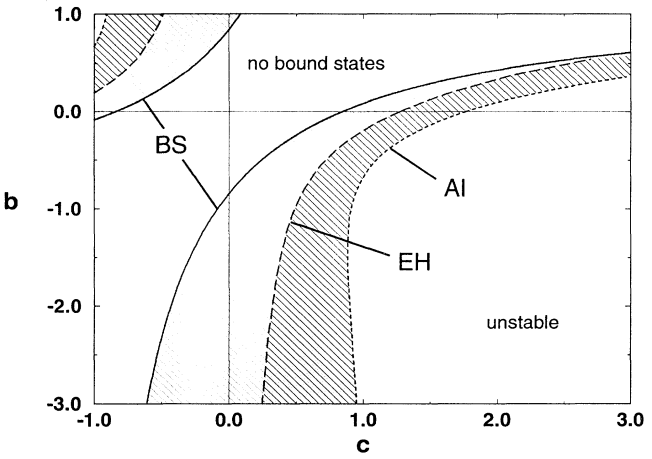

FIG. 6. The borders of existence of bound states for oppositely charged spirals. The solid line is given by the expression (48). The boundary of convective (EH) and absolute instability (AI) for the waves emitted by spiral are also shown (for explanation see [19]).

fore all the results concerning the structure of the eigenfunctions and the characteristic roots remain the same. Then the critical value $c_{\rm cr}$ corresponds to a curve in the b-c plane

$$\frac{c-b}{1+bc} = c_{\rm cr} \approx 0.845. \tag{48}$$

This curve defines the border of existence of bound states for oppositely charged spirals. It is plotted in Fig. 6 (curve BS). Also included in Fig. 6 is the Eckhaus-stability boundary (curve EH) and the boundary of absolute stability (curve AI) for the waves emitted by the spirals. The Eckhaus instability signals the onset of convective instability [19].

Since the full equation (9) is not invariant under the similarity transformation, the velocities and the equilibrium distances cannot be determined in this way. Then a calculation along the lines of Secs. III and IV including b from the beginning on is necessary.

C. The case $b = c$

For the case $b = c$ Eq. (6) can be simplified significantly because then $\psi = 0$ [see Eq. (3)], leading to

$$\Delta W - \frac{\Delta_r F}{F} W + \frac{2i}{r^2}\partial_\theta W - F^2(W + W^*) - \frac{\mathbf{v}\nabla W + i\mathbf{v}\nabla(\theta)W}{1+ib} = \frac{v}{1+ib}\left(F'\sin(\theta+\eta) + i\frac{F}{r}\cos(\theta+\eta)\right). \tag{49}$$

The boundary conditions are simply $\partial_x W = 0$ for $x = 0$ for oppositely charged spirals.

Consider first the case $b = 0$. Separating the real and imaginary parts of (49) one obtains

$$\Delta A - \frac{\Delta_r F}{F} A - \frac{2}{r^2} B_\theta - 2F^2 A - \mathbf{v}\nabla A + \mathbf{v}\nabla(\theta) B = vF'\sin(\theta+\eta),$$

$$\Delta B - \frac{\Delta_r F}{F} B + \frac{2}{r^2} A_\theta - \mathbf{v}\nabla B - \mathbf{v}\nabla(\theta) A = v\frac{F}{r}\cos(\theta+\eta). \tag{50}$$

For $r \gg 1$ one can neglect the terms $\sim r^{-2}$ and $\sim \mathbf{v}\nabla(\theta)W$, leading to the equations

$$\Delta A - 2F^2 A - \mathbf{v}\nabla A = 0,$$

$$\Delta B - \mathbf{v}\nabla B = \frac{v}{r}\cos(\theta+\eta). \tag{51}$$

Actually, the second equation in (51) coincides exactly with the phase diffusion equation obtained in [14]. It is well known that in the region $vr \gg 1$ the term $\sim \mathbf{v}\nabla B$ is very important because it provides a cutoff at large r. Introducing the new variable $\tilde{B} = B - \theta$ we have

$$\Delta\tilde{B} - \mathbf{v}\nabla\tilde{B} = 0, \tag{52}$$

which is the same as in [14]. The important result is that, due to the interaction, the motion of the vortices is purely radial. According to Ref. [17] the velocity obeys roughly the following expansion:

$$\ln(v_0/v) = \exp(\pm vr/2)[K_0(vr/2) \pm K_1(vr/2)],$$

$$v_0 = 3.29 \tag{53}$$

where the + sign corresponds to a like-charged pair, the − sign to an oppositely charged one, and K_0 and K_1 are modified Bessel functions. Comparison with full simulations shows that the accuracy of (53) is not very high [20].

For the case $b = c \neq 0$ the vortices acquire also a tangential component of the velocity. Nevertheless, also for this case no bound states exist. This follows from the fact that for $b = c$ the CGLE can be represented in the generalized potential form

$$\frac{\partial a}{\partial t} = -(1+ib)\frac{\delta H}{\delta a^*}, \tag{54}$$

with the potential $H = -\int dxdy(-|a|^2 + |\nabla a|^2 + |a|^4/2)$. From (54) it immediately follows that

$$\frac{\partial H}{\partial t} = -\frac{2}{(1+b^2)}\int dxdy|\partial_t a|^2 \leq 0. \tag{55}$$

Therefore on the trajectories of Eq. (1) the quantity H, which is bounded from below, can only decrease. This should also hold for the uniformly moving bound state because for this uniformly translating solution the potential H cannot depend on time explicitly (obviously a static solution does not exist). This result is in contradiction to [21], where the perturbations around the case

$b = c$ are considered. The bound states found in that paper are the result of the inapplicability of the method for small distances. Actually, the equilibrium distance according to the results of the paper is even smaller than the radius of the core.

In the nonlinear Schrödinger limit $b \to \infty$ we clearly have energy conservation and it is known that oppositely charged defects drift without radiation at the distance fixed by the initial conditions [22] (possibly this solution does not exist at small distance).

D. Interaction of like-charged spirals

For large separation X the interaction of like-charged spirals is similar to the interaction of oppositely charged ones. The only difference is that for the like-charged case both components of the velocities of the spirals have opposite sign, whereas for the oppositely charged case the tangential components have the same sign. This causes the rotation of the spirals around the common center of the symmetry in the like-charged case. To see the similarity we note that for small x and $|y| \ll X$ one has approximately $a(x,y) = a(x,-y)$ [this can be explained from Eqs. (19)–(21)]. Thus the symmetry $a(x,y) = a(-x,-y)$ (like-charged) and $a(x,y) = a(-x,y)$ (oppositely charged) have nearly the same effect on the boundary conditions. This result is in good agreement with simulations. For $|b-c|$ below the critical value one has repulsion at large distance (as in the oppositely charged case) and at small distance. So it is quite clear that the interaction is repulsive everywhere.

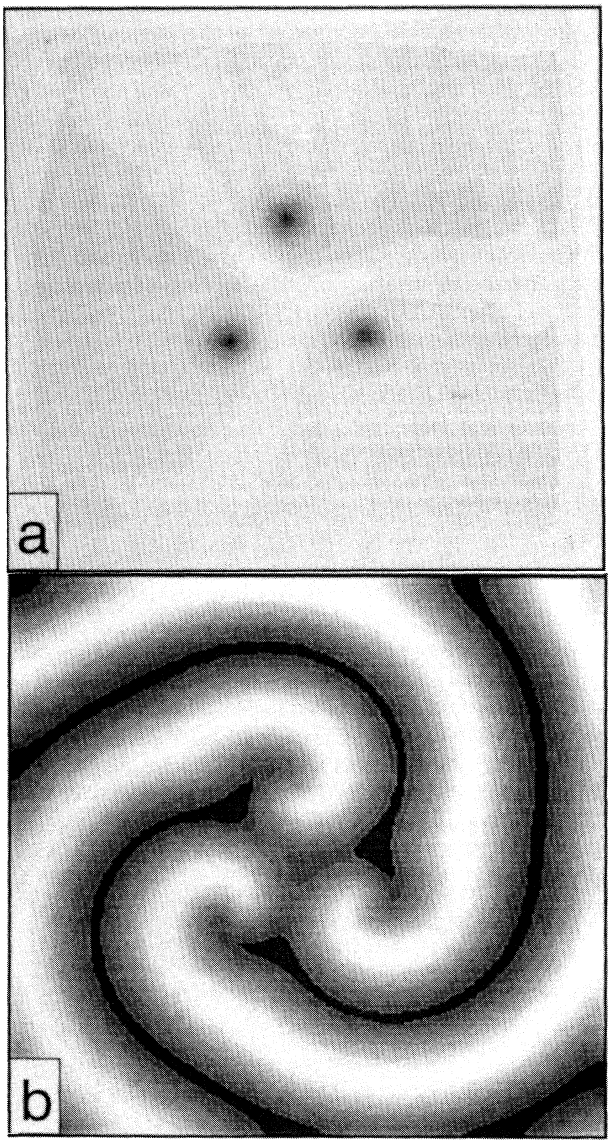

FIG. 7. The bound state of three like-charged spirals for $b = 0, c = 1.4$ in a 60×60 domain. Represented: (a) $|a(x,y)|$; (b) $\mathrm{Re}a(x,y)$.

Like-charged spirals may form more complicated bound states or aggregates. Such a bound state of three like-charged spirals is presented in Fig. 7. In contrast to the two-spiral bound states, which are simply rotating with constant velocity, each spiral in the aggregate performs a more complicated motion (possibly nonperiodic) on the background of a steady-state rotation. An interesting question is: What is the maximal number of spirals in an aggregate as a function of the parameters of the CGLE?

VI. CONCLUSION

Although our treatment explains the qualitative features of the bound states, the quantitative discrepancy in Fig. 3(b) indicates that there is room for improvement. Possibly the inclusion of $1/r$ corrections, which we dropped after Eq. (20), can clear up this point. Also, the correct inclusion of the shock structure, where the waves emitted from neighboring spirals collide, may have quantitative relevance.

An interesting result of this work is that the interaction of spirals at sufficiently large distance is either oscillatory, leading to stable bound states, or else presumably repulsive (this was verified numerically only for one set of parameters). Therefore in the parameter range where isolated spirals are stable (see Fig. 6) one may expect that in an ensemble of well-separated spirals annihilation does not occur, although it is not obvious that our results carry over to ensembles. We should point out that the shock is not necessarily situated symmetrically between spirals, but asymmetric states (stationary or very long lived) are possible. Drastic asymmetries develop spontaneously when the interaction between neighboring spiral pairs become important (lattice of spirals). Then one has a situation where only one type of defect (with one topological charge) emits spiral waves whereas their counterparts get trapped in the shock structures [19, 16]. Our simulations in fact indicate that in the convectively unstable range extended lattices of spirals with global topological charge zero exist only in the asymmetric state.

In this paper we considered the stable range of the parameters (see Fig. 6). Below the line AI the individual spirals lose stability and spatiotemporal chaos (defect-mediated turbulence) is established [23, 19]. In this range spontaneous creation and annihilation of the spirals takes

place with a well-defined average density of the defects. One can speculate on the possible relevance of our results for that case.

It is also possible that the results presented here are important in 3D. In this case the basic structures are scrolls, vortex rings, and scrolled vortices (see, e.g., [24]). One can expect that existence of the stable bound states in 2D is a necessary condition for the stability of vortex rings.

Presumably the mechanism that is responsible for the formation of the bound states can operate also in excitable media and there is in fact some evidence from numerical simulations [25, 26]. We plan to apply our analysis to appropriate models. Moreover, target patterns [27] could exhibit similar effects, although in this case one does not expect a tangential velocity. Finally, the relation to a different class of spirals, which seems to arise in some stationary, isotropic pattern-forming systems, is a challenging question [28, 29].

ACKNOWLEDGMENTS

One of us (I.A.) wishes to thank the Alexander-von-Humboldt foundation for support and the University of Bayreuth for its hospitality. Support by the German–Israeli Foundation (GIF) and Deutsche Forschungsgemeinschaft (SFB 213, Bayreuth) is gratefully acknowledged.

[1] I.S. Aranson, L. Kramer, and A. Weber, Physica D **53**, 376 (1991).
[2] L. Pismen and A.A. Nepomnyashchy, Physica D **54**, 183 (1992).
[3] V.N. Biktashev, in *Nonlinear Waves II*, edited by A.V. Gaponov-Grekhov and M.I. Rabinovich, Research Reports in Physics (Springer, Heidelberg, 1989), p. 87.
[4] See, e.g., S.C. Müller, T. Plesser, and B. Hess, Physica D **24**, 71 (1987); G.S. Skinner and H.L. Swinney, *ibid.* **48**, 1 (1991).
[5] S. Jakubith, H.H. Rotermund, W. Engel, A. von Oertzen, and G. Ertl, Phys. Rev. Lett. **65**, 3013 (1990); K. Krischer, M. Eiswirth, and G. Ertl, Surf. Sci. **251/252**, 900 (1991); A. Karma and X. Zou, Phys. Rev. A **46**, 3083 (1992).
[6] R.W. Walden, P. Kolodner, A. Passner, and C.M. Surko, Phys. Rev. Lett. **55**, 496 (1985); E. Moses and V. Steinberg, Phys. Rev. A **34**, 693 (1986); I. Rehberg and G. Ahlers, Phys. Rev. Lett. **55**, 500 (1985).
[7] H. Lekkerkerker, J. Phys. (Paris) Lett. **38**, 277 (1977); Q. Feng, W. Decker, W. Pesch, and L. Kramer, J. Phys. (Paris) II **2**, 1303 (1992).
[8] I. Rehberg, S. Rasenat, and V. Steinberg, Phys. Rev. Lett. **62**, 756 (1989); I. Rehberg, B.L. Winkler, M. de la Torre Juarez, S. Rasenat, and W. Schöpf, in *Festkörperprobleme: Advances in Solid State Physics* (Vieweg, Braunschweig, 1989), Vol. 29.
[9] P.C. Hohenberg and M. Cross, Rev. Mod. Phys. (to be published).
[10] F.T. Arecchi, G. Giacomelli, P.L. Ramazza, and S. Residori, Phys. Rev. Lett. **65**, 2531 (1990); **67**, 3749 (1991); Ch. Tamm, L.A. Lugiato, M. Bramabilla, A.B. Coates, C.O. Weiss, and R. McDuff, in *Dynamics and Quantum Effects in Nonlinear Optical Systems* (Springer-Verlag, Berlin, 1991).
[11] A.C. Newell, Lect. Appl. Math. **15**, 157 (1974).
[12] Y. Kuramoto and S. Koga, Prog. Theor. Phys. **66**, 1081 (1981); Y. Kuramoto, *Chemical Oscillations, Waves and Turbulence*, Springer Series in Synergetics (Springer-Verlag, Berlin, 1984).
[13] W.F. Loomis, *The Development of Dictyostelium Discoideum* (Academic, New York, 1987); J.M. Davidenko, P. Kent, and J. Jalife, Physica D **49**, 182 (1991).
[14] E. Bodenschatz, L. Kramer, and W. Pesch, Physica D **32**, 135 (1988).
[15] L. Kramer and A. Weber, J. Stat. Phys. **64**, 1007 (1991).
[16] E. Bodenschatz, M. Kaiser, L. Kramer, W. Pesch, A. Weber, and W. Zimmermann, in *New Trends in Nonlinear Dynamics and Pattern Forming Phenomena: The Geometry of Nonequilibrium*, Vol. 237 of *NATO Advanced Study Institute, Series B*, edited by P. Coullet and P. Huerre (Plenum, New York, 1990), p. 111; E. Bodenschatz, A. Weber, and L. Kramer, in *Nonlinear Processes in Excitable Media*, Vol. 244 of *NATO Advanced Study Institute, Series B: Physics*, edited by A.V. Holden, M. Markus, and H.G. Othmer (Plenum, New York, 1990).
[17] D. Rodriguez, L. Pismen, and L. Sirovich, Phys. Rev. A **44**, 7980 (1991).
[18] P.S. Hagan, SIAM J. Appl. Math **42**, 762 (1982).
[19] I. Aranson, L. Aranson, L. Kramer, and A. Weber, Phys. Rev. A **46**, 2992 (1992); A. Weber, L. Kramer, I.S. Aranson, and L.B. Aranson, Physica D **61**, 279 (1992).
[20] A. Weber, Ph.D. Thesis, University of Bayreuth, Germany, 1992 (unpublished).
[21] C. Matsuoka and K. Nozaki, J. Phys. Soc. Jpn. **61**, 1429 (1992).
[22] T. Creswick and N. Morrison, Phys. Lett. A **76**, 267 (1980); J. Nue, Physica D **43**, 385 (1990); L.M. Pismen and J. Rubinstein, Physica D **47**, 353 (1991).
[23] P. Coullet, L. Gil, and J. Lega, Phys. Rev. Lett. **62**, 1619 (1989).
[24] A.T. Winfree and S.H. Strogatz, Physica D **8**, 35 (1983); **9**, 65 (1983); **9**, 335 (1983); A.V. Panfilov and A.T. Winfree, *ibid.* **17**, 323 (1985).
[25] E.A. Ermakova, A.M. Pertsov, and E.E. Shnol, Physica D **40**, 185 (1989).
[26] A.T. Winfree, *When Time Breaks Down* (Princeton University Press, Princeton, 1987).
[27] J.J. Tyson and J.P. Keener, Physica D **32**, 327 (1988).
[28] E. Bodenschatz, J.R. de Bruyn, G. Ahlers, and D.S. Cannell, Phys. Rev. Lett. **67**, 3078 (1992).
[29] A. Buka, H. Richter, B. Winkler, and I. Rehberg (private communication).

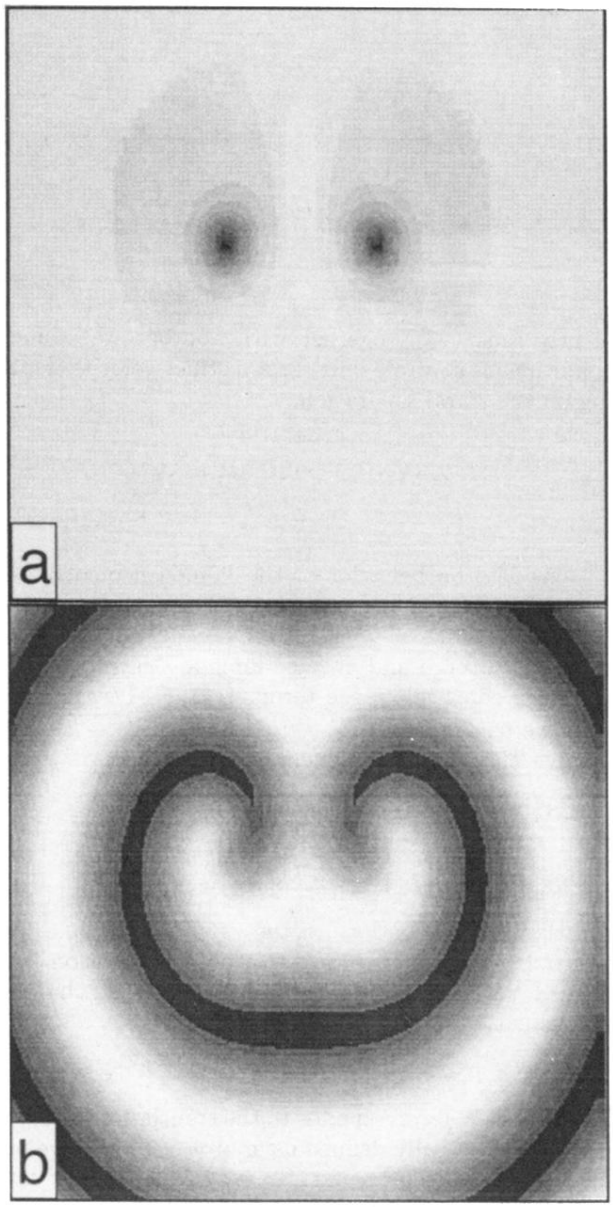

FIG. 1. The bound state of oppositely charged spirals for $b = 0, c = 1.5$ in a 100×100 domain. Represented: (a) $|a(x, y)|$; (b) real part $\mathrm{Re}a(x, y)$. Snapshot is coded in the grey scale, maximum of the field corresponds to black, minimum to white.

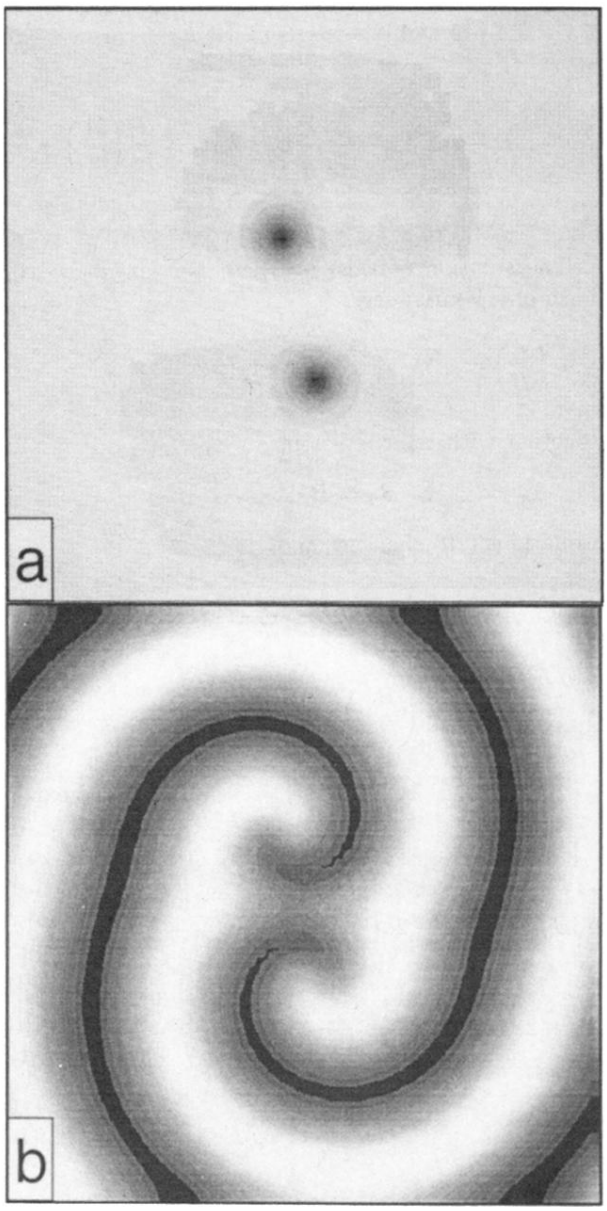

FIG. 2. The bound state of two like-charged spirals for $b = 0, c = 1.5$ in a 50×50 domain. Represented: (a)$|a(x, y)|$; (b) Re$a(x, y)$.

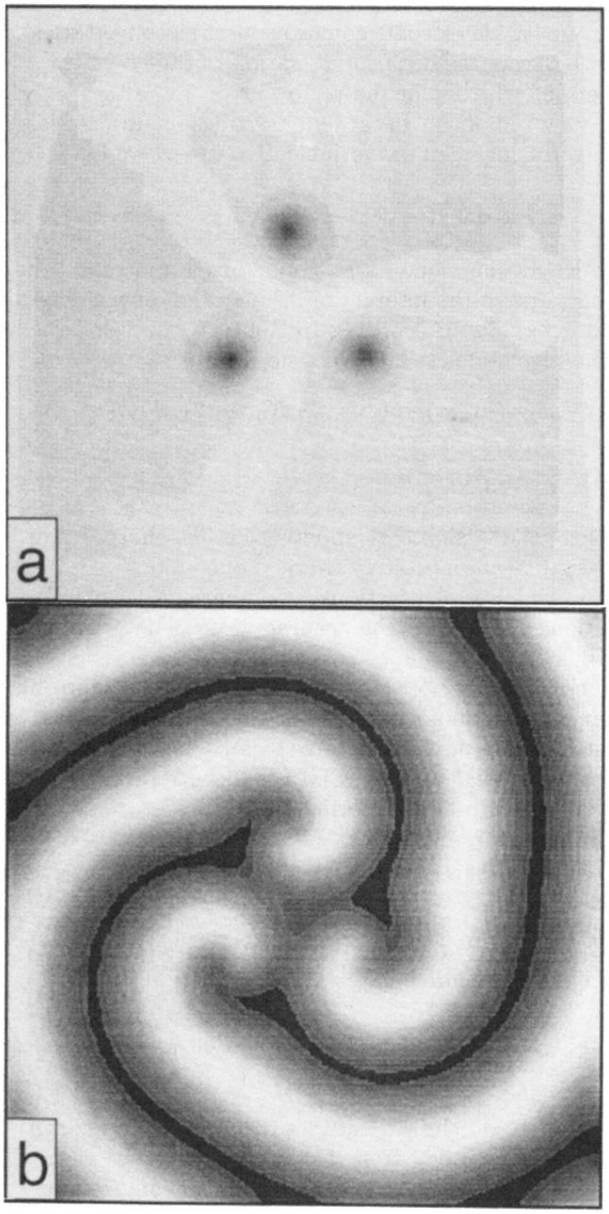

FIG. 7. The bound state of three like-charged spirals for $b = 0, c = 1.4$ in a 60×60 domain. Represented: (a) $|a(x, y)|$; (b) $\mathrm{Re}a(x, y)$.